Published in final edited form as:
Immunity. 2009 August 21; 31(2): 232–244. doi:10.1016/j.immuni.2009.06.022.

A role for lipid bodies in the cross-presentation of phagocytozed antigens by MHC class I in dendritic cells

Laurence Bougneres[1,*], **Julie Helft**[1,*], **Sangeeta Tiwari**[2,*], **Pablo Vargas**[1], **Benny Hung-Junn Chang**[3], **Lawrence Chan**[3], **Laura Campisi**[4], **Gregoire Lauvau**[4], **Stephanie Hugues**[1], **Pradeep Kumar**[2], **Alice O. Kamphorst**[5], **Ana-Maria Lennon Dumenil**[1], **Michel Nussenzweig**[5], **John D. MacMicking**[2,§], **Sebastian Amigorena**[1,§], and **Pierre Guermonprez**[1,5,§]

[1]INSERM U653, Institut Curie, Section Recherche, 26, rue d'Ulm, 75248 Paris, Cedex 05, France

[2]Microbial Pathogenesis, Boyer Centre for Molecular Medicine, Yale University School of Medicine, New Haven, CT 06510, USA

[3]Baylor College of Medicine, One Baylor Plaza, Houston, TX 77030, USA

[4]IPMC, INSERM U924, 06560 Valbonne, France.

[5]Rockefeller University, Laboratory of Molecular Immunology, 1230 York Avenue, New York, NY 10065, USA

Summary

Dendritic cells (DCs) have the striking ability to cross-present exogenous antigens in association with MHC class I to CD8+ T cells. However, the intracellular pathways underlying cross-presentation remain ill-defined. Current models involve cytosolic proteolysis of antigens by the proteasome and TAP-dependent import into Endoplasmic Reticulum (ER) or phagosomal lumen. Here, we show that DCs express an ER-resident 47kDa immune-related GTPase, Irgm3. Irgm3 resides on ER and lipid body (LB) membranes where it binds the LB coat component ADRP. Genetic removal of either Irgm3 or ADRP leads to defects in LB formation in DCs and severely impairs cross-presentation of phagocytozed antigens to $CD8^+$ but not antigen presentation to CD4+ T cells. We thus define a new role for LB organelles in regulating cross-presentation of exogenous antigens to CD8+ T lymphocytes in DCs.

Introduction

DCs are highly specialized antigen presenting cells endowed with the ability to prime or tolerize antigen-specific naïve T cells (Steinman et al., 2003). CD8+ T cells recognize endogenous antigens (Ag) as short peptides associated to MHC I. Antigenic peptides arising from proteasomal degradation are translocated into the ER lumen by transporters associated with Ag processing (TAP1/2). Once in the ER, the peptides undergo amino terminal trimming by

Correspondence: Pierre Guermonprez, pguermonpr@mail.rockefeller.edu.
*,§These authors contributed equally to work

The authors have no conflicting financial interests.

ERAP amino peptidases and are loaded on neo-synthesized MHC I molecules by a complex, which is composed of calreticulin, tapasin and ERp57 (Cresswell et al., 2005).

DCs can also present exogenous Ag in association with MHC I by a process called “cross-presentation” (Cresswell et al., 2005). Ag uptake by macropinocytosis (Norbury et al., 1997), receptor-mediated endocytosis (Bonifaz et al., 2002; Regnault et al., 1999) or phagocytosis (Kovacsovics-Bankowski and Rock, 1995) all initiate efficient cross-presentation.

Despite the importance of cross-presentation in tolerance and infectious immunity (Steinman et al., 2003; Steinman and Nussenzweig, 2002), the cellular pathways underlying this process are not fully understood. In most experimental systems, cross-presentation relies on cytosolic processing events since it can be blocked by pharmacological inhibition of the proteasome and requires functional TAP transporters (Kovacsovics-Bankowski and Rock, 1995). Indeed, there is considerable evidence that exogenous Ag can access the cytosol after phagocytosis (Kovacsovics-Bankowski and Rock, 1995), macropinocytosis (Norbury et al., 1997) or receptor-mediated endocytosis (Bonifaz et al., 2002; Rodriguez et al., 1999). The mechanisms underlying the delivery of Ag to the cytosol are ill-understood but may involve the ERAD pathway, which targets mis-folded, lumenal ER proteins to proteasomal degradation (Ackerman et al., 2006). Nevertheless, it remains unclear whether ERAD-mediated retro-translocation operates from the ER (after retrograde transport of endocytosed Ag) (Ackerman et al., 2005) or from the endocytic pathway (after recruitment of ER to endosomes and phagosomes) (Ackerman et al., 2003; Burgdorf et al., 2008; Guermonprez et al., 2003; Houde et al., 2003). In addition, a wealth of evidence supports the idea that cross-presentation is also favoured by the low proteolytic activity of the endocytic pathway in DCs (Hotta et al., 2006; Lennon-Dumenil et al., 2002; Savina et al., 2006). Finally, DEC-205 or mannose receptor-dependent retention of Ag in the early endocytic pathway favors cross-presentation (Bonifaz et al., 2002; Burgdorf et al., 2007; Burgdorf et al., 2008). However, the precise coordination of endocytic and cytosolic events leading to Ag proteolysis and MHC I loading during cross-presentation remains to be established.

Therefore, it is crucial that we begin to identify the molecular components of the transport pathways that control cross-presentation. GTPases are natural candidates, since they act as major regulators of intracellular traffic. Among those with dedicated immune function is a new family of 47kDa immunity-related GTPases (p47 GTPases) related to the dynamin superfamily and regulating vesicular trafficking (MacMicking, 2004; Shenoy et al., 2007). Recent genetic analysis has established that p47 GTPases exert pathogen-specific immunity to infectious agents occupying a vacuolar niche in both human and mouse settings (MacMicking, 2004; Shenoy et al., 2007). One p47 GTPase in particular, Irgm3 (IGTP), was found to reside extensively within the ER (Taylor et al., 1996; Taylor et al., 1997) and is critical for interferon (IFN)-dependent immunity to *Toxoplasma gondii* (Ling et al., 2006; Taylor et al., 2000). However, whether Irgm3 contributes to adaptive immunity remains unknown.

In this study, we show that Irgm3 controls cross-presentation in DCs. We find that Irgm3-deficient DCs exhibit a major impairment in their ability to cross-present phagocytic Ag to CD8+ but not to present Ag to CD4+ T cells. The role of Irgm3 in the cross-presentation pathway relies on intracellular events, since Irgm3-deficient DCs still phagocytose Ag particles and interact with T cells with the same efficiency as their WT counterparts. We demonstrate that Irgm3 localizes to ER membranes but also, unexpectedly, to lipid bodies (LBs). LBs (also called lipid droplets) are neutral lipid storage organelles composed of a central core of cholesteryl esters and triglycerides surrounded by a single layer of phospholipids which are thought to originate from ER membranes (Fujimoto et al., 2008). Irgm3 controls LB accumulation in DCs after activation both *in vitro* and *in vivo*. Complementation of Irgm3-deficient DCs by retroviral infection restores both LBs and efficient cross-presentation, which

suggests that LBs have a direct effect on cross-presentation. In addition, we show that pharmacological inhibition of diacylglycerol acyltransferase decreases LB accumulation in DC and inhibits cross-presentation. ADRP belongs to the group of PAT-domain containing proteins that regulate LB biogenesis and dynamics (Brasaemle, 2007; Brasaemle et al., 1997; Chang et al., 2006; Fujimoto et al., 2008). We identified the LB coat protein ADRP as a partner of Irgm3: Irgm3 physically interacts and co-localizes with ADRP in LBs in DCs. This interaction is functionally relevant since accumulation of LB driven by Irgm3 requires ADRP. Finally, genetic inactivation of ADRP markedly inhibits both LB accumulation and cross-presentation of phagocytosed Ag by DCs.

Taken together, these results identify LBs as key organelles that regulate cross-presentation of phagocytosed Ag in DCs.

Results

Irgm3 expression in DCs

Previous studies have shown that the expression of Irgm3 is uniformly low in various cell types and further increased by IFN exposure (MacMicking et al., 2003; Taylor et al., 2000; Taylor et al., 1996). Thus we wanted to determine whether Irgm3 is expressed in DCs. Using RT-PCR and immunoblot (IB), we found constitutive expression of Irgm3 in monocyte derived DCs (mDCs, Figure 1A). IFN-γ induced a dramatic increase in Irgm3 expression in mDCs (Figure 1A). Significantly, the basal level of both Irgm3 mRNA and protein was 10 fold higher in untreated mDCs as compared to bone marrow-derived macrophages (Figure 1A, $p<0.0001$ and Figure 1B, $p<0.005$). Moreover, Irgm3 mRNA and protein was detected in both CD8+ and CD8− DCs purified from mouse spleen (Figure 1A and C). Finally, injection of the IFN-inducer polyI:C in mice led to an increase of Irgm3 protein (Figure 1C). In conclusion, Irgm3 is constitutively expressed by DCs and further increased upon activation.

Role of Irgm3 in cross-presentation

We found that Irgm3 deficiency does not impair the differentiation of mDCs in GM-CSF dependent cultures, their cell surface phenotype or their ability to respond to LPS (Figure S1B).

To examine the contribution of Irgm3 in Ag presentation, mDCs were pulsed with ovalbumin (OVA) coated latex beads for 20 minutes, washed, chased for five hours and fixed before incubation with OVA-specific CD8+ OT-I transgenic T cells whose activation was monitored by CD69 upregulation. As shown in Figure 1D, *Irgm3*−/− mDCs were unable to efficiently cross-present OVA Ag after latex bead phagocytosis. Indeed, a 4-fold increase in OVA concentration on the beads was required to reach the same efficiency of cross-presentation as compared to control mDCs (Figure 1D). In line with the normal expression of MHC I and costimulatory molecules (Figure SD1), *Irgm3*−/− mDCs are not impaired in their ability to activate OT-I T cells after pulsing with OVA MHC I peptide (Figure 1E). Next we explored the possibility that *Irgm3*−/− mDCs were also defective for the MHC II Ag presentation pathway. We found that *Irgm3*−/− mDCs were equivalent as WT mDCs in their ability to activate OVA specific OT-II transgenic CD4+ T cell following OVA latex beads phagocytosis or OVA MHC II peptide loading (Figure 1F and G). These results indicate that *Irgm3*−/− mDCs have a selective defect for cross-presentation *in vitro*, while MHC II-restricted Ag presentation is unaffected.

To assess the contribution of Irgm3 to cross-presentation by lymphoid organs DCs *in vivo*, WT or *Irgm3*−/− mice were injected subcutaneously with OVA coupled to an anti-DEC205 (Bonifaz et al., 2002). As shown in Figure 1H, cross-presentation of targeted OVA to adoptively transferred OT-I T cells was slightly but significantly reduced in *Irgm3*−/− mice

when compared with their WT counterparts ($p<0.001$). *Ex vivo* sorting of total lymphoid organ DCs loaded *in vivo* with anti-DEC-OVA conjugates (or high doses of soluble OVA) and *in vitro* co-culture with OT-I T cells further confirmed that *Irgm3*−/− deficient DCs display slightly reduced cross-presentation *in situ* (SD2, 3). The contribution of Irgm3 to normal cross-presentation in these systems; however, is smaller than it is in mDCs (see above). To examine the role of Irgm3 in phagocytic cross-presentation by activated DCs, we compared the ability of WT and *Irgm3*−/− mice to cross-prime endogenous CD8+ T cells after intravenous injection of apoptotic bodies loaded with OVA+polyI:C (Schulz et al., 2005). PolyI:C, a viral double-stranded RNA mimetic recognized by TLR-3, increases Irgm3 levels in splenic DCs (Figure 1C). As shown in Figure 1I, T cell cross-priming of endogenous CD8+ T cells was decreased in *Irgm3*−/− mice when compared with WT mice ($p<0.005$).

To assess the ability of *Irgm3*−/− mice to mount an endogenous CD8+ T cell response, we infected WT or *Irgm3*−/− mice with *Listeria monocytogenes* secreting OVA in the cytosol of infected cells. We found no significant difference in the activation of OVA-specific polyclonal CD8+ T cells in WT and *Irgm3*−/− mice (SD4). We conclude that the CD8+ T cell compartment is normal in *Irgm3*−/− mice, and that their DCs are competent to present OVA if large quantities of this Ag are delivered into the cytosol directly.

Taken together, these results identify Irgm3 as a positive regulator of cross-presentation *in vitro* and *in vivo*.

Irgm3 does not control phagocytosis but does delay phagosomal maturation

To begin dissecting the mechanism underlying the role of Irgm3 in cross-presentation, we analyzed phagosomal function in *Irgm3*−/− mice.

First we assessed the efficiency of Irgm3 deficient mDC in performing phagocytosis, using a stringent FACS-based assay quantifying only internalized beads (SD5). Control and *Irgm3*−/− deficient mDCs display the same efficiency of phagocytosis (Figure 2A). We conclude that Irgm3 is not involved in the phagocytosis of latex beads. Accordingly, Ag presentation by MHC II is not impaired in Irgm3 deficient mDCs (Figure 1F).

Since Irgm3 does not impact the efficiency of Ag uptake, we hypothesized that Irgm3 might modify phagosomal maturation.

Despite Irgm3 localization to ER (Taylor et al., 1997), we did not observe any difference in the transient association of calnexin to early phagosomes from control or *Irgm3*−/− mDCs (Ackerman et al., 2003; Gagnon et al., 2002; Guermonprez et al., 2003; Houde et al., 2003) (data not shown).

Next we tested whether Irgm3 controls the dynamics of phagolysosomal maturation. Control or *Irgm3*−/− mDCs were incubated with OVA-cross linked latex beads for 10 minutes, washed and their phagosomes were analyzed at various time points by FACS. We found that phagosomes from *Irgm3*−/− mDCs exhibit an accelerated acquisition of the phagolysosomal marker LAMP2, as well as an increased degradation of phagosomal OVA (Figure 2B and C). We therefore conclude that Irgm3 acts a negative regulator of phagosomal maturation.

Irgm3 localizes to the ER and LBs

To gain further insight into the intracellular mechanisms underlying Irgm3 involvement in cross-presentation, we first investigated the subcellular distribution of Irgm3 in IFN-γ treated mDCs by immunofluorescence (IF). As previously shown in other cell types (Taylor et al., 1997), a small percentage of Irgm3 colocalized with calnexin-positive ER, including perinuclear membrane (Figure 3A, Linescan 1). Much more pronounced staining; however,

was noted on spherical cytosolic donut-shaped structures of large size (0.5–2μm), completely devoid of calnexin (Figure 3A, Linescan 2).

MHC I staining revealed a strong accumulation in the perinuclear area characteristic of Golgi apparatus, but did not colocalize with the Irgm3-bright vesicles (Figure 3B). Using mDCs from MHC II-GFP knockin mice (Boes et al., 2002); we did not find any colocalization between the Irgm3-bright vesicles and MHC II positive compartments (Figure 3C). Lastly, Irgm3-bright vesicles did not stain with the endo-lysosomal marker LAMP1 (Figure 3D) nor with endocytic compartments labeled with 10kD fluorescent dextran tracers that had been chased for 20 minutes and followed up to 240 minutes post-uptake (Figure 3E).

Thus Irgm3-bright vesicles are not ER, MHC I or II transport vesicles, nor intermediates of the endocytic network. Because of their morphology, we hypothesized that these vesicles were lipid bodies (LB) or lipid droplets. A striking feature of LBs is that they are comprised of a dense hydrophobic core of neutral lipids, surrounded by a hemi-membrane that do not support the insertion of transmembrane proteins (Fujimoto et al., 2008). The lipophilic dye Bodipy 493/503 (Bodipy) specifically stains the neutral lipids that form the core of the LB. Using this probe, we identified Irgm3-bright structures as LBs (Figure 4A). Usually, Irgm3 LBs are localized in the periphery of the cells and are sometimes close to or in direct contact with the perinuclear ER (Figure 4A). The cores of the LBs were stained with Bodipy while Irgm3 was concentrated at the periphery of these organelles (Figure 4B). Irgm3 localization to LBs increases with LBs numbers (SD6). Therefore, LBs represent a new intracellular localization for Irgm3, in addition to the previously described ER localization.

Since phagosomal maturation and phagocytic cross-presentation are dependent on Irgm3, we sought to determine whether Irgm3 could also be recruited to phagosomes. We did not detect any strong recruitment of Irgm3 in phagosomes from mDCs at any time points after phagocytosis (up to 240 minutes, Figure 4C). In contrast, we often found Irgm3/Bodipy positive LBs contacting phagosomes (20.9% at 60 min phagocytic pulse, Figure 4C, D). The percentage of phagosomal association decreased slightly after three hours of phagosomal maturation reaching 14.3% of the phagosomes (Figure 4D).

In summary, Irgm3 is mostly associated with LBs. This finding led us to investigate the possibility that Irgm3 controls LB accumulation in DCs.

Irgm3 controls LB accumulation in DCs

To quantify LB accumulation under basal conditions, WT and *Irgm3*−/− mDCs were stained with Bodipy (Figure 5A). We found that the number of LBs per cell was significantly decreased in *Irgm3*−/− when compared to control mDCs (Figure 5A; median WT: 1 vs *Irgm3*−/−: 0; $p<0.0001$). Twice as many *Irgm3*−/− mDCs are devoid of any LBs as compared to controls (SD7).

Since IFN-γ increases Irgm3 expression (Figure 1), we tested the effect of IFN-γ treatment on LBs accumulation. We found a major increase in the median number of LBs in IFNγ-treated mDCs as compared to untreated WT mDCs (Figure 5A; median WT:1 vs WT+IFN-γ: 6). This increase is almost completely lost in the absence of Irgm3 (Figure 5A; median +IFN-γ WT: 6 vs *Irgm3*−/−:1; $p<0.0001$). *Irgm3*−/− mDCs were not able to accumulate more than 10 LBs per cell (SD7, middle panel). These findings demonstrate that Irgm3 is a major regulator of LB accumulation in IFN-γ–activated mDCs.

In order to determine whether LBs accumulate in the conditions of our cross-presentation assays, we counted LBs in mDCs exposed to OVA-coated latex beads. We found a significant increase in LBs in OVA-coated latex bead-exposed WT mDCs as compared to controls (Figure

5A, median WT:1 vs WT +OVA-beads: 5). OVA-beads dependent increase is almost completely absent in the case of *Irgm3*−/− mDCs (Figure 5A, median *Irgm3*−/−: 0 vs *Irgm3* −/− +OVA-beads: 1). In addition, *Irgm3*−/− mDCs exposed to beads accumulated only up to five LBs per cell, whereas many control mDCs harbored more than 15 LBs per cell (SD7, lower panel).

To obtain larger sample quantitation of LB accumulation, we analysed Bodipy-labeled DCs by FACS. This method measures the LB amount at the single cell level in a large number of cells. As shown in Figure 5B, the Bodipy signal was slightly higher in control mDCs when compared to *Irgm3*−/− mDCs. Significantly, the increase in LB accumulation in IFN-γ-induced or latex bead-pulsed WT mDCs was not observed in the absence of Irgm3 (Figure 5B).

In splenic DCs, we observed that CD8+ DCs have more LBs than their CD8− counterparts in WT mice (Figure 5C, 37% reduction, $p<0.0001$). This data is compatible with the idea that LBs may participate in cross-presentation, since CD8+ DCs are more efficient than their CD8 − counterparts in cross-presentation of phagocytosed Ag (den Haan et al., 2000; Iyoda et al., 2002; Schnorrer et al., 2006). *Irgm3*−/− DCs exhibit a slight defect in LB accumulation both in CD8+ subset ($p<0.05$) and CD8− subset ($p<0.005$). Activation induced by *in vivo* injection of polyI:C induced efficient maturation both in control and *Irgm3*−/− mice (SD8), and also induced Irgm3 expression in control mice (Figure 1C). PolyI:C induced a net increase in the LB accumulation of CD8+ DCs ($p<0.005$) and, to a lesser extent, in the CD8− DCs ($p<0.05$) (Figure 5C). By contrast, *Irgm3*−/− DCs were unable to increase LB accumulation in response to polyI:C in both subsets. As a result, the difference between control and *Irgm3*−/− DCs increased after activation, leading to a 47% reduction in the CD8+ subset ($p<0.05$) and a 66% reduction in the CD8− subset ($p<0.05$) (Figure 5C).

Collectively, our results clearly demonstrate that Irgm3 plays a significant role in the establishment of the LB pool in DCs. Irgm3 induction promotes LB accumulation after DC stimulation (mDCs after IFN-γ, polyI:C in splenic DCs). Irgm3-dependent effects appear specific for immune stimulation since the induction of LBs by oleic acid feeding is not compromised in *Irgm3*−/− mDCs, which suggests that the basal LB producing machinery is not impaired in *Irgm3*−/− cells (SD10).

These results identify Irgm3 as an immune regulator of LB accumulation and suggest that LBs may facilitate cross-presentation.

LBs are required for normal cross-presentation

The results presented so far show a role for Irgm3 in both cross-presentation and the control of LB accumulation in DCs. These findings led us to investigate the possibility that a connection exists between these two processes.

To distinguish whether Irgm3 impacts the cross-presentation by altering mDC development, we reintroduced Irgm3 in Irgm3−/−DCs. Retrovirally transduced Irgm3−/−mDCs expressed the protein which localized to LBs and increased LB levels (Figure 6A, B and C).

To test whether Irgm3 complementation would restore cross-presentation, we retrovirally transduced *Irgm3*−/− mDCs pulsed 30mn with OVA-coated beads. After six hours, cells were washed and incubated with OT-I T cells overnight. As shown in figure 6F, the cross-presentation defect of *Irgm3*−/− mDCs is partially corrected by the *Irgm3* encoding virus, but not the control virus. We conclude that the effect of Irgm3 on cross-presentation is independent of any additional unknown effect that it might have on DC development.

To determine whether the LB accumulation in DC correlates with the efficiency of cross-presentation, we compared mDCs that were distinct in their LB accumulation but identical in Ag load. mDCs harboring one OVA-bead were FACS-sorted according to their "low" or "high" LB accumulation and co-cultured with OT-I T cell for 18 hrs (Figure 6E). We found far more efficient cross-presentation within the LB "high" population even though the two DC populations expressed similar levels of CD86 and activated OT-I T cells upon OVA MHC I peptide loading similarly (Figure 6F, SD9). We conclude that the total intracellular accumulation of LBs measured by Bodipy fluorescence correlates with cross-presentation by mDCs.

To further probe the requirement of LBs in cross-presentation, we designed a second approach aimed at reducing LB levels by inhibiting Acyl CoA:diacylglycerol acyltransferase (DGAT), which produces triglycerides stores. Xanthohumol has been identified as a DGAT inhibitor (Tabata et al., 1997). mDCs were fed with OVA-coated latex beads or pulsed with OVA MHC I peptide during 30mn, washed and then cultured for four hours with Xanthohumol at 85 μM, which resulted in a 30–50% inhibition of LB as measured by FACS (Figure 6G, SD11). Cells were then washed and fixed before overnight incubation with OT-I T cells. Xanthohumol inhibited cross-presentation of OVA-coated latex beads by 44% at the highest dose of beads and by 51% at the lowest dose of beads ($p<0.001$ in both cases) but left unaffected the presentation of the OVA peptide (Figure 6 H, I).

These experiments confirm that LBs are required for normal cross-presentation by mDCs *in vitro*.

ADRP interacts with Irgm3 and is required for LB formation and cross-presentation

The way in which Irgm3 exerts its effects on LB biogenesis remains unclear. However, recent yeast 2-hybrid analysis found that another p47 IRG, Irgd (IRG-47), interacts with the LB PAT protein ADRP (Yamaguchi et al., 2006). Loss of ADRP results in decreased LB formation in hepatocytes and macrophages (Brasaemle et al., 1997; Chang et al., 2006; Fujimoto et al., 2008; Paul et al., 2008). We found that ADRP is expressed in mDCs and colocalizes on the same LBs as Irgm3 (Figure 7A). To investigate the possibility that the two proteins interact directly, we performed pull-down assays using GST-Irgm3 as bait. ADRP was immunoprecipitated efficiently with GST-Irgm3 but not with GST-Irgm1, GST or glutathione beads alone (Figure 7B). Reciprocally, Myc-tagged ADRP immunoprecipitated Irgm3 and the positive control, Irgd, but not Irgm1 in mammalian cell extracts (Figure 7B). Notably, interaction between Irgm3 and ADRP did not require Irgm3 GTPase activity; a constitutive GDP-bound Irgm3 mutant ($Irgm3^{S98N}$) still immunoprecipitated ADRP (SD12). These findings fit with earlier observations showing that $Irgm3^{S98N}$ remains associated to membranes, suggesting that GTPase activity is not required for steady-state localization (Taylor et al., 1997).

Having identified ADRP as a partner for Irgm3, we next asked whether genetic lesions in Adrp phenocopy those of Irgm3. In contrast to *Irgm3−/−*, *Adrp−/−* mDCs exhibited a strongly decreased level of LB even before activation (42 % of decrease in Bodipy MFI, $p<0.005$, Figure 6C) and a reduced induction of LBs upon oleate feeding (SD10). Since Irgm3 controls the up-regulation of LB accumulation upon IFN-γ exposure (Figure 5), we sought to analyze the LB accumulation of *Adrp−/−* cells after IFN-γ treatment. We found that IFN-γ treated *Adrp−/−* mDCs failed to upregulate LBs as their WT counterparts (Figure 6D, $p<0.0001$). This result was confirmed by LB counting in IF after Bodipy staining (Figure 7E): after IFN-γ treatment, the average number of LB was reduced from 6.4 LB/cell in WT versus 3.1/cell in *Adrp−/−* ($p<0.0001$). We conclude that LB accumulation after IFN-γ treatment is dependent on ADRP, which interacts with Irgm3.

Previous studies identified a greater than 10-fold enrichment of ADRP mRNA in CD8+ as compared to the CD8− spleen DC subset (Dudziak et al., 2007; Edwards et al., 2003). At the protein level, we found a two-fold enrichment of ADRP in the CD8+ DC subset when compared to the CD8− DC subset (IB, Figure 7F; $p<0.05$). Consistent with this observation, ADRP positive LBs were abundant in CD8+ DC; in addition, Irgm3 and ADRP colocalized on the same LBs (SD13).

We found that *Adrp*−/− splenic DCs are defective in LB accumulation, and even more so than *Irgm3*−/− DCs (Figure 7G). We conclude that ADRP is required for LB accumulation in splenic DCs.

To determine whether the loss of ADRP altered cross-presentation by splenic DCs, we compared OVA-bead cross-presentation assays with WT, *Irgm3*−/− and *Adrp*−/− splenic DCs. As shown in Figure 7H, OT-I T cells activation was decreased two-fold when they were activated by *Adrp*−/− or *Irgm3*−/− DCs, as compared to WT control. ADRP deficiency had no effect on cell surface phenotype, nor on phagocytic ability, nor on the ability to present OVA peptide to CD8+ T cells, nor on DC maturation (SD 14 and data not shown).

These experiments establish the convergence of Irgm3 and ADRP-containing LBs as a regulatory organelle for the cross-presentation pathway in DCs from lymphoid organs.

Discussion

The present study identifies an IFN-inducible ER-resident GTPase, Irgm3, as a new component of the cross-presentation pathway. Irgm3-defective DCs fail to cross-present phagocytozed Ag efficiently, while interaction with T cells, phagocytosis and presentation to CD4+ T cells remain unaffected. Therefore, Irgm3 controls some cellular events required for efficient cross-presentation. In addition to its documented residence in the ER (Taylor et al., 1997), we show that Irgm3 associates with compartments distinct from the ER or endosome. Two characteristics define these vesicles as LBs: a) a dense core of neutral lipids stained by the LB-specific probe Bodipy, b) an outer envelope covered with the LB-specific coat protein ADRP. LBs are storage organelles for neutral lipids such as cholesteryl esters or triglycerides (Fujimoto et al., 2008). ADRP is sufficient to activate *de novo* formation of LBs in adipocytes as well as other cell types when over-expressed (Gao and Serrero, 1999). The removal of ADRP leads to hepatic and macrophage LB deficiency *in vivo* (Chang et al., 2006; Paul et al., 2008).

We found that Irgm3 controls the accumulation of LBs induced by cell activation following various stimuli (IFN-γ or polyI:C). This induction appears to involve ADRP that physically associates with Irgm3 during IFN-γ-induced upregulation of LBs. Irgm3 may participate in the neoformation of LBs by regulating the association of ADRP with the LB outer membrane. Alternatively, it may help stabilize a pre-existing interaction of ADRP with LBs since Irgm3 itself does not appear to bind neutral lipids directly (Tiwari et al., 2009). This latter interaction could prevent the recruitment of cytosolic lipases (Brasaemle, 2007).

We provide several lines of evidence that show that LBs are involved in cross presentation: *First*, activation of LB accumulation upon Irgm3 retroviral complementation increases cross-presentation in *Irgm3*−/− mDCs.

Second, depletion of LB by pharmacological inhibition of DGAT inhibits cross-presentation in WT mDCs.

Third, ADRP deficiency leads to decreased LB accumulation and decreased cross-presentation. ADRP is very specifically associated with LBs (Brasaemle et al., 1997). In this respect, the fact that *both* Irgm3 and ADRP are needed for cross-presentation—two proteins structurally

and phylogenetically dissimilar to one another—is likely to be explained on the basis of their dual action at the level of LBs. This interpretation is further reinforced by these proteins almost exclusive co-localization to LBs and their ability to physically interact *in vitro* and *in vivo*.

In conclusion, three independent loss-of-function approaches that perturb LB homeostasis—two genetic, one pharmacologic—also disrupt cross-presentation in DCs. Moreover, complementation or gain-of-function of at least one of these components, Irgm3, overturns such defects. These data identify LBs as a positive regulator of the cross-presentation pathway in DCs.

How and where do LBs exert their effects on the cross-presentation pathway?

Irgm3 and Irga6, are both ER-associated p47 GTPases that have been proposed to disrupt *Toxoplasma gondii* parasitophorous vacuoles by triggering membrane vesiculation and fission (Ling et al., 2006; Martens et al., 2005). We did not observe any strong association to phagosomes, or any membranolytic activity of recombinant Irgm3 on synthetic membranes (SD15). This finding does not support the idea that Irgm3 promotes cross-presentation through a direct destabilization of phagosomal membranes enabling the delivery of phagosomal Ag to the cytosol.

It has been proposed that the process of LB neoformation may also promote the formation of transient lipidic pores at the level of ER membranes (Ploegh, 2007). This could be in relation to the established function of LBs as cytosolic sites for ubiquitinylation of ER-derived proteins (Fujimoto and Ohsaki, 2006). Further studies are required to determine whether these processes underlie the effect of Irgm3 and ADRP on cross-presentation of phagocytozed Ag.

Here we show that Irgm3 negatively effects phagosomal maturation both in terms of late marker acquisition (LAMP2) and proteolytic activity (OVA degradation). Thus, besides other mechanisms, the action of Irgm3 may participate in the establishment of endocytic compartment endowed with a low proteolytic activity favouring crosspresentation (Delamarre et al., 2005; Hotta et al., 2006; Lennon-Dumenil et al., 2002; Savina et al., 2006; Trombetta et al., 2003). The phagosome-LB contact sites that we have identified may support a regulatory function of LBs on phagolysosomal progression. Importantly, the negative effect of Irgm3 on phagolysosomal progression is in line with its lack of involvement in anti-mycobacterial innate immunity, which relies on the activation of phagolysosomal function (MacMicking et al., 2003).

LBs have already been described in DCs, including in the first description of these cells (Maroof et al., 2005; Steinman and Cohn, 1973). Our results have uncovered a completely new aspect of DC biology, related to lipid metabolism and its implication for Ag cross-presentation by MHC I. Further studies are required to identify the molecular pathways controlling the involvement of LBs in cross-presentation in DCs.

Experimental procedures

See supplementary methods for details.

Mice

Irgm3-deficient mice (Taylor et al., 2000), *Adrp*-deficient mice (Chang et al., 2006), OVA-specific CD8+ (OT-I) an CD4+ (OT-II) TCR transgenic mice, MHC II-GFP knockin mice (Boes et al., 2002) have been described previously.

Cells and Ag presentation assays

Bone marrow-derived GM-CSF DCs (day 7–8) were used and termed as mDCs. For some experiments, Irgm3 expression was induced by 3–5 hours treatment with 250ng/ml IFN-γ. Spleen DCs (SDCs) were isolated from mouse spleens after collagenase digestion and purified using CD11c magnetic beads (Miltenyi) and further purified by FACS sorting. *In vitro* cross-presentation assays were adapted from procedures previously described (Guermonprez et al., 2003) and used CD69 up-regulation in OT-I T cells as a readout. For some experiments, mDCs were infected with pMx retrovirus harbouring Irgm3 cDNA (or control empty retrovirus) in the presence of polybrene (10μg/ml). DEC-OVA conjugates were prepared as previously described (Bonifaz et al., 2002). For *in vivo* cross-priming assay 30.10^7 splenic cells from β2m-deficient mice were loaded endocytically by pulsing with 20mg/ml OVA plus 2mg/ml polyI:C for 15mn prior γ irradiation and iv injection. Eight days later, spleens were harvested and IFN-γ production by endogenous CD8+ T cells was measured after peptide specific restimulation.

Phagosome assays

For flow cytometric analysis of phagosomes, 25.10^6 DCs were pulsed for 10 min at 37°C at a ratio of 1:3 with 3μm latex beads coupled covalently to OVA by glutaraldehyde cross linking. Then, cells were washed three times on a serum gradient at 150 G (4°C) before chase at 37°C. After hypoosmotic lysis and fixation, phagosomes were stained with anti-OVA or anti-LAMP2 antibodies and analyzed by FACS (Guermonprez et al., 2003).

LBs measurements and immunofluorescences

After cell surface staining, cells were fixed with PFA 1%, and stained for LBs in PermWash solution (Becton Dickinson) with BOPIDY FL (Molecular probes) at 4μg/ml for FACS analysis and 10μg/ml for immunofluorescences.

GST pull down assays

Recombinant p47 GTPases expressing GST tAg were immobilized on gluthathione sepharose and incubated with HEK lysates of transiently expressed ADRP-myc for coimmunoprecipitation. In the reverse experiments, lysates of HEK cells transfected with Myc-ADRP and various EYFP-tagged p47 GTPases were immunoprecipitated with anti-Myc resin.

Supplementary Material

Refer to Web version on PubMed Central for supplementary material.

Acknowledgments

The authors thank G. Taylor, H. Shen, Z. Maciorowski, C. Guerin, I. Grandjean, A. Boissonnas, L. Saveanu, A. Savina, W. Faigle, D. Loew, B. Lombard, CL. Trubert, S. Davis for reagents, helping discussions or critical reading of the manuscript. LB was supported by ARC, Curie Institute and INSERM. LC was supported by the USA NIH Grant HL 51586. JDM was supported by NIH NIAID (R01 AI068041-01A1), BWF Award, Searle Foundation (05-F-114), CRI and W.W. Winchester Foundation. PG was supported by the CNRS, ANR and the Rockefeller University.

References

Ackerman AL, Giodini A, Cresswell P. A role for the endoplasmic reticulum protein retrotranslocation machinery during crosspresentation by dendritic cells. Immunity 2006;25:607–617. [PubMed: 17027300]

Ackerman AL, Kyritsis C, Tampe R, Cresswell P. Early phagosomes in dendritic cells form a cellular compartment sufficient for cross presentation of exogenous antigens. Proc Natl Acad Sci U S A 2003;100:12889–12894. [PubMed: 14561893]

Ackerman AL, Kyritsis C, Tampe R, Cresswell P. Access of soluble antigens to the endoplasmic reticulum can explain cross-presentation by dendritic cells. Nat Immunol 2005;6:107–113. [PubMed: 15592474]

Boes M, Cerny J, Massol R, Op den Brouw M, Kirchhausen T, Chen J, Ploegh HL. T-cell engagement of dendritic cells rapidly rearranges MHC class II transport. Nature 2002;418:983–988. [PubMed: 12198548]

Bonifaz L, Bonnyay D, Mahnke K, Rivera M, Nussenzweig MC, Steinman RM. Efficient targeting of protein antigen to the dendritic cell receptor DEC-205 in the steady state leads to antigen presentation on major histocompatibility complex class I products and peripheral CD8+ T cell tolerance. J Exp Med 2002;196:1627–1638. [PubMed: 12486105]

Brasaemle DL. Thematic review series: adipocyte biology. The perilipin family of structural lipid droplet proteins: stabilization of lipid droplets and control of lipolysis. J Lipid Res 2007;48:2547–2559. [PubMed: 17878492]

Brasaemle DL, Barber T, Wolins NE, Serrero G, Blanchette-Mackie EJ, Londos C. Adipose differentiation-related protein is an ubiquitously expressed lipid storage droplet-associated protein. J Lipid Res 1997;38:2249–2263. [PubMed: 9392423]

Burgdorf S, Kautz A, Bohnert V, Knolle PA, Kurts C. Distinct pathways of antigen uptake and intracellular routing in CD4 and CD8 T cell activation. Science 2007;316:612–616. [PubMed: 17463291]

Burgdorf S, Scholz C, Kautz A, Tampe R, Kurts C. Spatial and mechanistic separation of cross-presentation and endogenous antigen presentation. Nat Immunol 2008;9:558–566. [PubMed: 18376402]

Chang BH, Li L, Paul A, Taniguchi S, Nannegari V, Heird WC, Chan L. Protection against fatty liver but normal adipogenesis in mice lacking adipose differentiation-related protein. Mol Cell Biol 2006;26:1063–1076. [PubMed: 16428458]

Cresswell P, Ackerman AL, Giodini A, Peaper DR, Wearsch PA. Mechanisms of MHC class I-restricted antigen processing and cross-presentation. Immunol Rev 2005;207:145–157. [PubMed: 16181333]

Delamarre L, Pack M, Chang H, Mellman I, Trombetta ES. Differential lysosomal proteolysis in antigen-presenting cells determines antigen fate. Science 2005;307:1630–1634. [PubMed: 15761154]

den Haan JM, Lehar SM, Bevan MJ. CD8(+) but not CD8(−) dendritic cells cross-prime cytotoxic T cells in vivo. J Exp Med 2000;192:1685–1696. [PubMed: 11120766]

Dudziak D, Kamphorst AO, Heidkamp GF, Buchholz VR, Trumpfheller C, Yamazaki S, Cheong C, Liu K, Lee HW, Park CG, et al. Differential antigen processing by dendritic cell subsets in vivo. Science 2007;315:107–111. [PubMed: 17204652]

Edwards AD, Chaussabel D, Tomlinson S, Schulz O, Sher A, Reis e Sousa C. Relationships among murine CD11c(high) dendritic cell subsets as revealed by baseline gene expression patterns. J Immunol 2003;171:47–60. [PubMed: 12816982]

Fujimoto T, Ohsaki Y. Proteasomal and autophagic pathways converge on lipid droplets. Autophagy 2006;2:299–301. [PubMed: 16921266]

Fujimoto T, Ohsaki Y, Cheng J, Suzuki M, Shinohara Y. Lipid droplets: a classic organelle with new outfits. Histochem Cell Biol 2008;130:263–279. [PubMed: 18546013]

Gagnon E, Duclos S, Rondeau C, Chevet E, Cameron PH, Steele-Mortimer O, Paiement J, Bergeron JJ, Desjardins M. Endoplasmic reticulum-mediated phagocytosis is a mechanism of entry into macrophages. Cell 2002;110:119–131. [PubMed: 12151002]

Gao J, Serrero G. Adipose differentiation related protein (ADRP) expressed in transfected COS-7 cells selectively stimulates long chain fatty acid uptake. J Biol Chem 1999;274:16825–16830. [PubMed: 10358026]

Guermonprez P, Saveanu L, Kleijmeer M, Davoust J, Van Endert P, Amigorena S. ER-phagosome fusion defines an MHC class I cross-presentation compartment in dendritic cells. Nature 2003;425:397–402. [PubMed: 14508489]

Hotta C, Fujimaki H, Yoshinari M, Nakazawa M, Minami M. The delivery of an antigen from the endocytic compartment into the cytosol for cross-presentation is restricted to early immature dendritic cells. Immunology 2006;117:97–107. [PubMed: 16423045]

Houde M, Bertholet S, Gagnon E, Brunet S, Goyette G, Laplante A, Princiotta MF, Thibault P, Sacks D, Desjardins M. Phagosomes are competent organelles for antigen cross-presentation. Nature 2003;425:402–406. [PubMed: 14508490]

Iyoda T, Shimoyama S, Liu K, Omatsu Y, Akiyama Y, Maeda Y, Takahara K, Steinman RM, Inaba K. The CD8+ dendritic cell subset selectively endocytoses dying cells in culture and in vivo. J Exp Med 2002;195:1289–1302. [PubMed: 12021309]

Kovacsovics-Bankowski M, Rock KL. A phagosome-to-cytosol pathway for exogenous antigens presented on MHC class I molecules. Science 1995;267:243–246. [PubMed: 7809629]

Lennon-Dumenil AM, Bakker AH, Maehr R, Fiebiger E, Overkleeft HS, Rosemblatt M, Ploegh HL, Lagaudriere-Gesbert C. Analysis of protease activity in live antigen-presenting cells shows regulation of the phagosomal proteolytic contents during dendritic cell activation. J Exp Med 2002;196:529–540. [PubMed: 12186844]

Ling YM, Shaw MH, Ayala C, Coppens I, Taylor GA, Ferguson DJ, Yap GS. Vacuolar and plasma membrane stripping and autophagic elimination of Toxoplasma gondii in primed effector macrophages. J Exp Med 2006;203:2063–2071. [PubMed: 16940170]

MacMicking JD. IFN-inducible GTPases and immunity to intracellular pathogens. Trends Immunol 2004;25:601–609. [PubMed: 15489189]

MacMicking JD, Taylor GA, McKinney JD. Immune control of tuberculosis by IFN-gamma-inducible LRG-47. Science 2003;302:654–659. [PubMed: 14576437]

Maroof A, English NR, Bedford PA, Gabrilovich DI, Knight SC. Developing dendritic cells become 'lacy' cells packed with fat and glycogen. Immunology 2005;115:473–483. [PubMed: 16011516]

Martens S, Parvanova I, Zerrahn J, Griffiths G, Schell G, Reichmann G, Howard JC. Disruption of Toxoplasma gondii parasitophorous vacuoles by the mouse p47-resistance GTPases. PLoS Pathog 2005;1:e24. [PubMed: 16304607]

Norbury CC, Chambers BJ, Prescott AR, Ljunggren HG, Watts C. Constitutive macropinocytosis allows TAP-dependent major histocompatibility complex class I presentation of exogenous soluble antigen by bone marrow-derived dendritic cells. Eur J Immunol 1997;27:280–288. [PubMed: 9022030]

Paul A, Chang BH, Li L, Yechoor VK, Chan L. Deficiency of adipose differentiation-related protein impairs foam cell formation and protects against atherosclerosis. Circ Res 2008;102:1492–1501. [PubMed: 18483409]

Ploegh HL. A lipid-based model for the creation of an escape hatch from the endoplasmic reticulum. Nature 2007;448:435–438. [PubMed: 17653186]

Regnault A, Lankar D, Lacabanne V, Rodriguez A, Thery C, Rescigno M, Saito T, Verbeek S, Bonnerot C, Ricciardi-Castagnoli P, Amigorena S. Fcgamma receptor-mediated induction of dendritic cell maturation and major histocompatibility complex class I-restricted antigen presentation after immune complex internalization. J Exp Med 1999;189:371–380. [PubMed: 9892619]

Rodriguez A, Regnault A, Kleijmeer M, Ricciardi-Castagnoli P, Amigorena S. Selective transport of internalized antigens to the cytosol for MHC class I presentation in dendritic cells. Nat Cell Biol 1999;1:362–368. [PubMed: 10559964]

Savina A, Jancic C, Hugues S, Guermonprez P, Vargas P, Moura IC, Lennon-Dumenil AM, Seabra MC, Raposo G, Amigorena S. NOX2 controls phagosomal pH to regulate antigen processing during crosspresentation by dendritic cells. Cell 2006;126:205–218. [PubMed: 16839887]

Schnorrer P, Behrens GM, Wilson NS, Pooley JL, Smith CM, El-Sukkari D, Davey G, Kupresanin F, Li M, Maraskovsky E, et al. The dominant role of CD8+ dendritic cells in cross-presentation is not dictated by antigen capture. Proc Natl Acad Sci U S A 2006;103:10729–10734. [PubMed: 16807294]

Schulz O, Diebold SS, Chen M, Naslund TI, Nolte MA, Alexopoulou L, Azuma YT, Flavell RA, Liljestrom P, Reis e Sousa C. Toll-like receptor 3 promotes cross-priming to virus-infected cells. Nature 2005;433:887–892. [PubMed: 15711573]

Shenoy AR, Kim BH, Choi HP, Matsuzawa T, Tiwari S, MacMicking JD. Emerging themes in IFN-gamma-induced macrophage immunity by the p47 and p65 GTPase families. Immunobiology 2007;212:771–784. [PubMed: 18086378]

Steinman RM, Cohn ZA. Identification of a novel cell type in peripheral lymphoid organs of mice. I. Morphology, quantitation, tissue distribution. J Exp Med 1973;137:1142–1162. [PubMed: 4573839]

Steinman RM, Hawiger D, Nussenzweig MC. Tolerogenic dendritic cells. Annu Rev Immunol 2003;21:685–711. [PubMed: 12615891]

Steinman RM, Nussenzweig MC. Avoiding horror autotoxicus: the importance of dendritic cells in peripheral T cell tolerance. Proc Natl Acad Sci U S A 2002;99:351–358. [PubMed: 11773639]

Tabata N, Ito M, Tomoda H, Omura S. Xanthohumols, diacylglycerol acyltransferase inhibitors, from Humulus lupulus. Phytochemistry 1997;46:683–687. [PubMed: 9366096]

Taylor GA, Collazo CM, Yap GS, Nguyen K, Gregorio TA, Taylor LS, Eagleson B, Secrest L, Southon EA, Reid SW, et al. Pathogen-specific loss of host resistance in mice lacking the IFN-gamma-inducible gene IGTP. Proc Natl Acad Sci U S A 2000;97:751–755. [PubMed: 10639151]

Taylor GA, Jeffers M, Largaespada DA, Jenkins NA, Copeland NG, Woude GF. Identification of a novel GTPase, the inducibly expressed GTPase, that accumulates in response to interferon gamma. J Biol Chem 1996;271:20399–20405. [PubMed: 8702776]

Taylor GA, Stauber R, Rulong S, Hudson E, Pei V, Pavlakis GN, Resau JH, Vande Woude GF. The inducibly expressed GTPase localizes to the endoplasmic reticulum, independently of GTP binding. J Biol Chem 1997;272:10639–10645. [PubMed: 9099712]

Tiwari S, Choi HP, Matsuzawa T, Pypaert M, MacMicking JD. Phagosomal membrane targeting of Irgm1 via PtdIns(3,4)P2 and PtdIns(3,4,5)P3 promotes mycobacterial immunity. Nature Immunology. 2009 In press.

Trombetta ES, Ebersold M, Garrett W, Pypaert M, Mellman I. Activation of lysosomal function during dendritic cell maturation. Science 2003;299:1400–1403. [PubMed: 12610307]

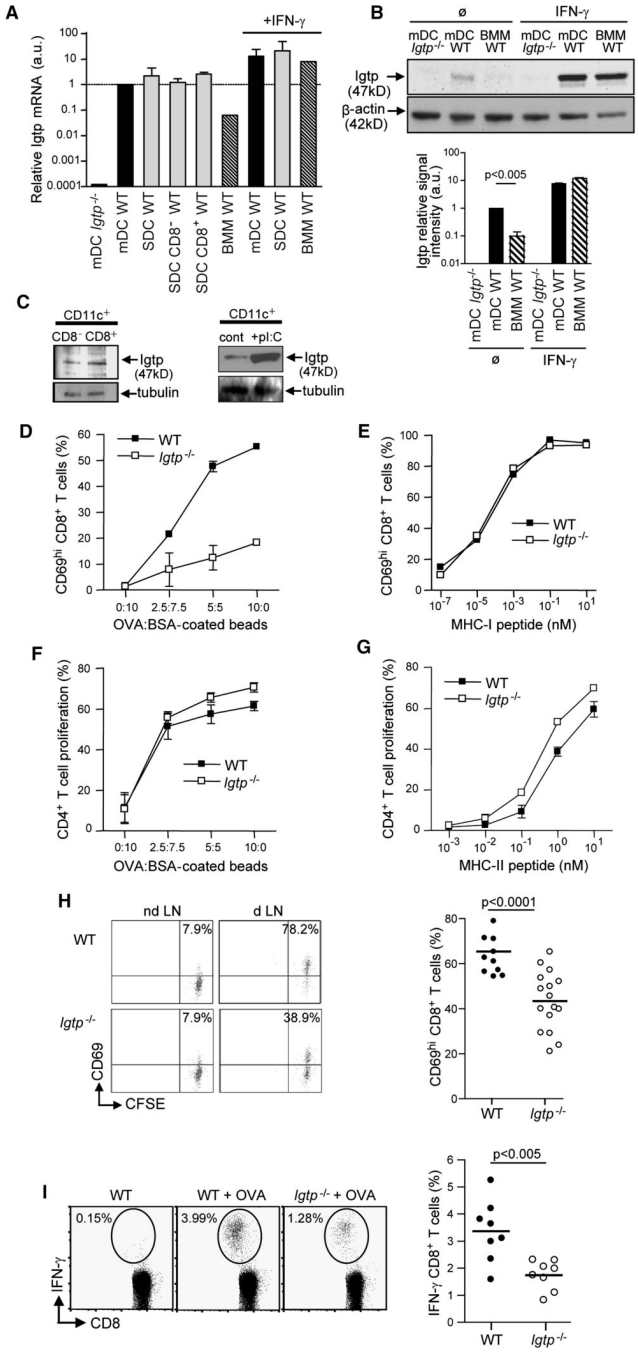

Figure 1. Irgm3 is expressed in DCs and regulates cross-presentation

(A) Relative Irgm3 mRNA expression in DCs (mDCs and Spleen DCs) and BMMs was measured by RT-PCR.

(B) IB analysis of Irgm3 expression in cell lysates from mDCs and BMMs. Densitometric quantification of Irgm3 signal intensity rapported to β-actin loading control.

(C) IB analysis of Irgm3 expression in cell lysates from CD11c+ spleen DCs subsets sorted on CD8 expression (upper panel) or total spleen DCs sorted 8 hours after the injection of 50 μg polyI:C (lower panel). α-tubulin is shown as a loading control.

(D, E) *In vitro* cross-presentation of OVA:BSA coated beads (D) and MHC I OVA peptide loading (E) by WT or *Irgm3*−/− mDCs. CD8+ T cell activation was determined by measuring CD69 upregulation after overnight incubation with fixed mDCs.
(F, G) *In vitro* MHC II presentation of OVA:BSA coated beads (F) and MHC II OVA peptide loading (G) by WT or *Irgm3*−/− mDCs. CD4+ T cell proliferation was determined by CFSE dilution after 3 days of coculture with fixed mDCs.
(H) *In vivo* cross-presentation after sc immunization of WT or *Irgm3*−/− mice with anti-DEC205-OVA. *In situ* cross presentation was monitored by CD69 upregulation in adoptively transferred anti-OVA OT-I transgenic cells at d1 (left panel). Results from three independent experiments are represented (right panel).
(I) *In vivo* cross-priming in WT or *Irgm3*−/− mice immunized with polyI:C and OVA-loaded apoptotic bodies. Anti-OVA polyclonal CD8+ T cell response was monitored at d8 after OVA peptide restimulation and IFN-γ intracellular staining (left panel). Data from three independent experiments are represented (right panel).

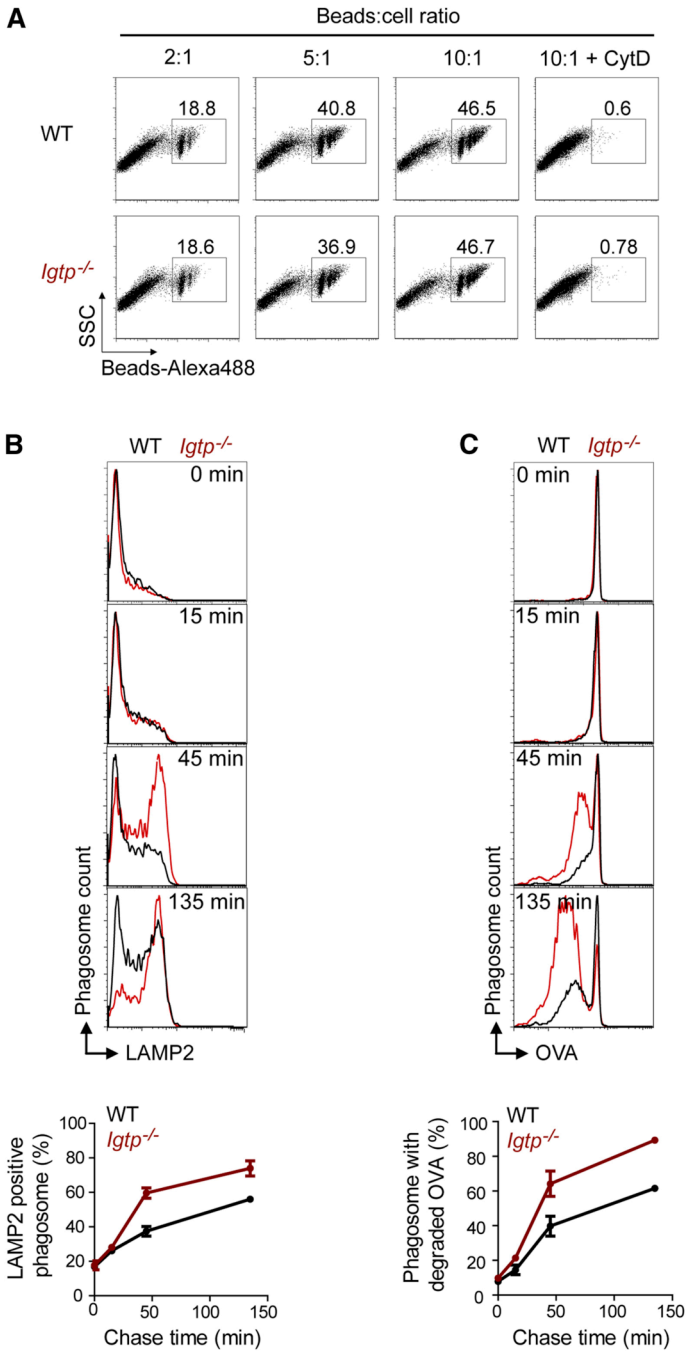

Figure 2. Irgm3 does not control phagocytosis but does delay phagosomal maturation

(A) Phagocytosis assay. WT or *Irgm3*−/− mDCs were incubated for 10 minutes with various amounts of latex beads labeled with Alexa-488 and analyzed by FACS in the presence of trypan blue to quench the fluorescence of extracellular beads. In the right panel, cells were pretreated with CytochalasinD to prevent phagocytosis.

(B, C) Phagosomal maturation assay. WT or *Irgm3*−/− mDCs were fed with OVA covalently linked to 3μm latex beads for 10mn, washed to remove free beads and left in culture for various time lapses. After hypoosmotic lysis and fixation, phagosomes were analyzed by flow cytometry after staining with anti-LAMP2 antibodies (B) or anti-OVA antibodies (C). A representative experiment is shown.

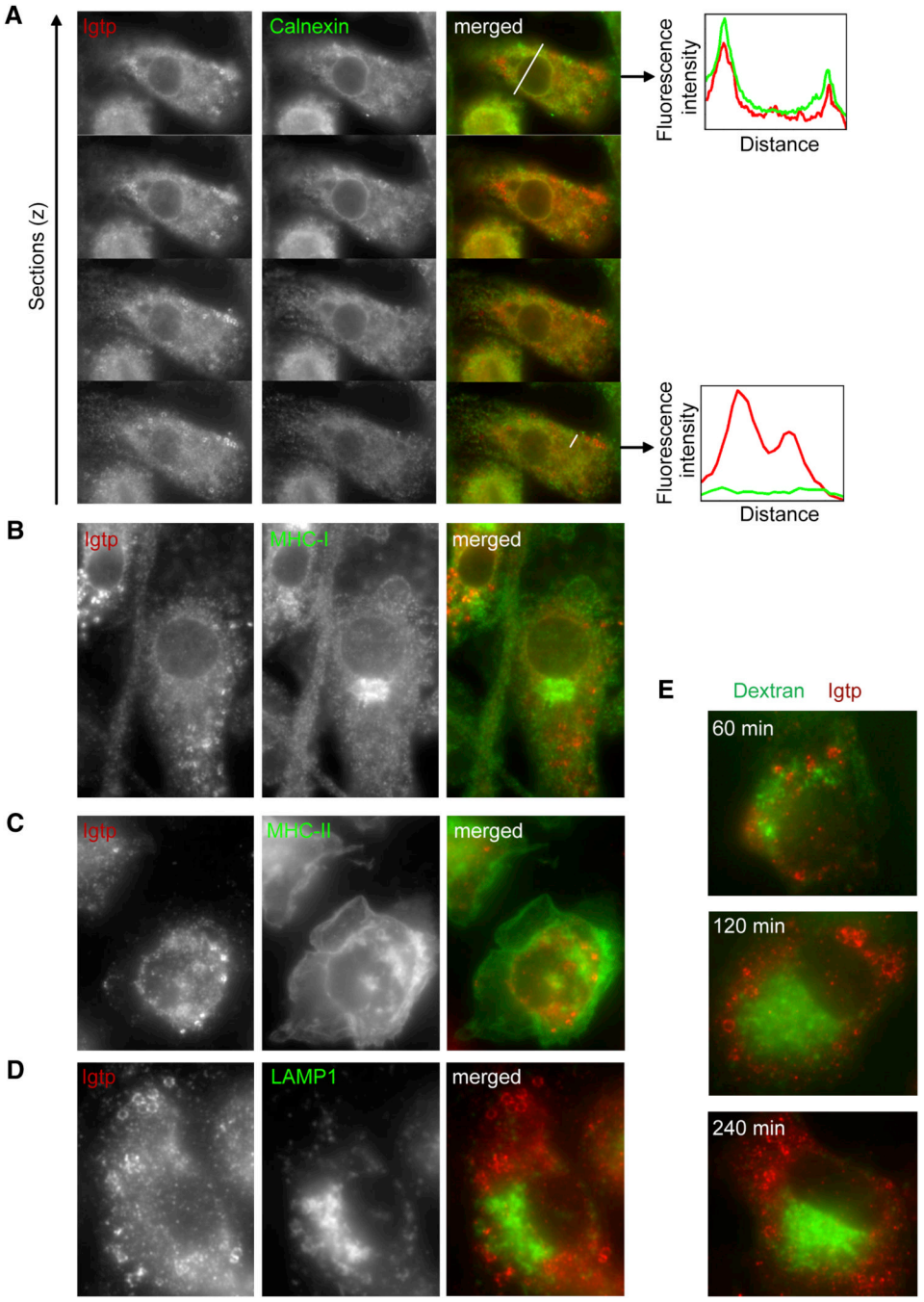

Figure 3. Irgm3 associates to ER and vesicles that are distinct from ER and endosomes

(A) Irgm3 colocalizes with calnexin at the ER and is associated to spherical cytosolic structures devoid of calnexin in IFN-γ treated WT mDCs. Graphs represent the quantification of Irgm3 (red line) and calnexin (green line) fluorescence intensity following the white lines drawn in the merged image.

(B) Irgm3-bright structures do not colocalize with H-2Kb MHC I in IFN-γ treated WT mDCs.

(C) Irgm3-bright structures do not colocalize with MHC II-GFP from MHC II-GFP knock in mice in IFN-γ treated mDCs.

(D) Irgm3-bright structures do not colocalize with LAMP1 in IFN-γ treated mDCs.

(E) Irgm3-bright structures are distinct from endocytic compartments accessible to exogenous 10 kD dextrans. Cells were pulsed for 20mn with fluorescent dextrans, extensively washed and left in culture for various time points before fixation.

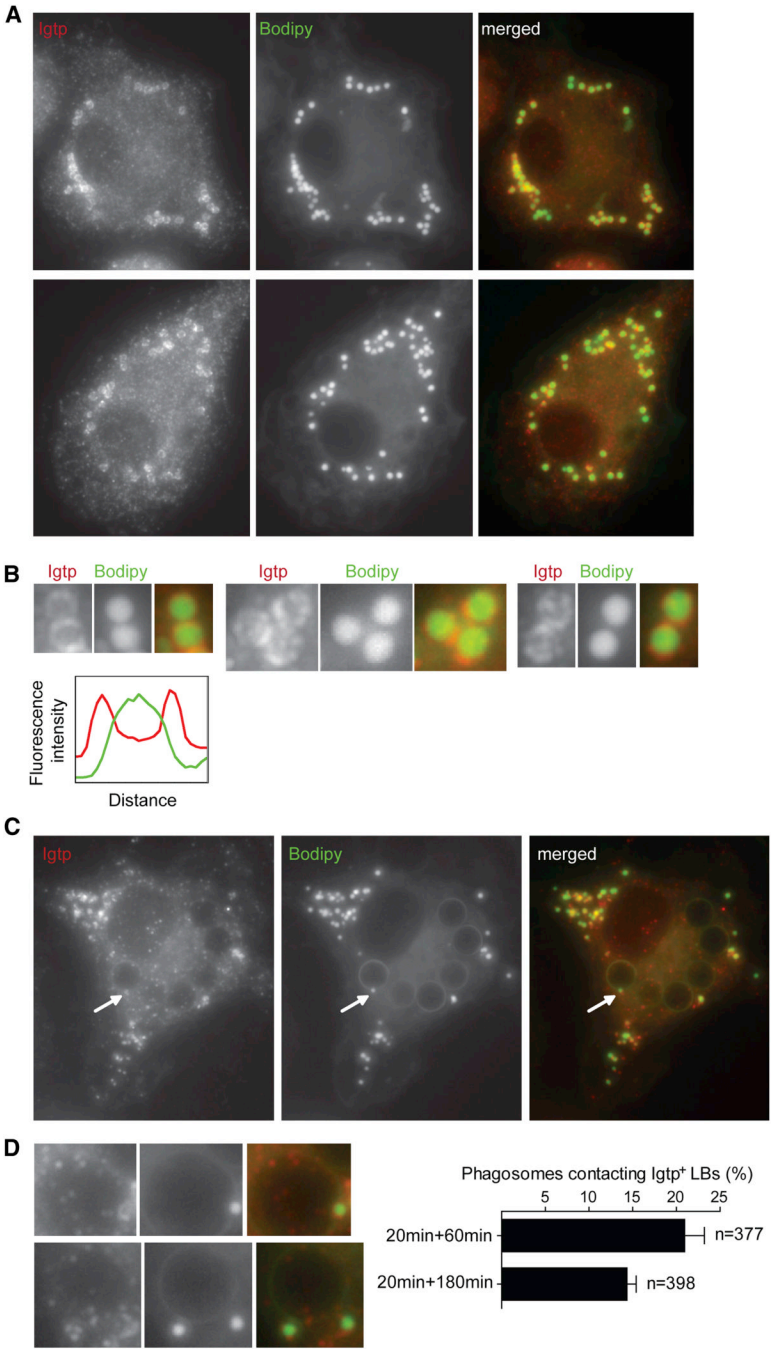

Figure 4. Irgm3 associates to LBs

(A) Irgm3 surrounds Bodipy positive lipid bodies (LBs). IFN-γ treated WT mDCs were fixed and stained with anti-Irgm3 antibody and the LB specific probe Bodipy.

(B) Detail of Irgm3 positive LB showing the surrounding ring of Irgm3 and the dense core of the LB stained with Bodipy. The graph represents the quantification of Irgm3 (red line) and Bodipy (green line) fluorescence intensity of a representative LB.

(C) WT mDCs were fed with 3μM latex beads for 30mn, then washed and cultured for 60min. Cells were fixed and the distribution of Irgm3-positive lipid bodies was analyzed by staining as in A.

(D) Detail of LB-phagosome contact sites. A quantification of phagosomes contacting Irgm3-positive LBs at two time points after the uptake of beads is shown.

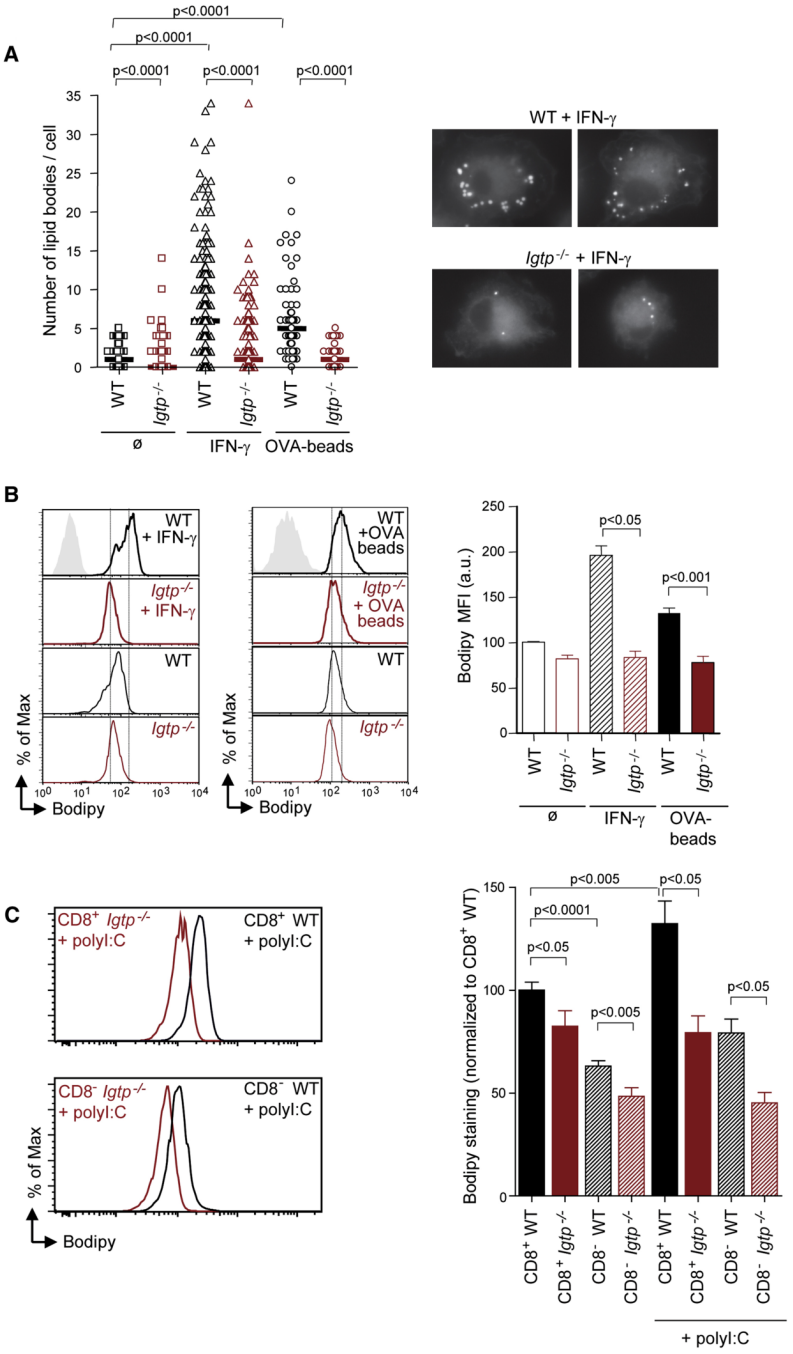

Figure 5. Irgm3 controls LBs accumulation in DCs

(A) Representative IF images of LB staining (Bodipy) in fixed WT or *Irgm3*−/− DCs after IFN-γ treatment. LBs were quantified in DCs. A representative experiment out of three is shown (70 to 200 cells were analyzed for each condition in each experiment). WT DCs or *Irgm3*−/− DCs, untreated or treated with IFN-γ, or pulsed with OVA-beads were analysed. Each symbol represents one cell section. Statistical significance was assessed using the Mann-Whitney test. (B) Bodipy FACS analysis of CD11c+ mDCs. WT (black lines) and *Irgm3*−/− DC (red lines) untreated, treated with IFN-γ, or pulsed with OVA-beads were analysed. Mean fluorescence intensity values of Bodipy staining from three independent experiments were normalized and

plotted as the average ± SEM (WT+IFN-γ MFI: 196±10 vs Irgm3−/+IFN-γ MFI: 84±7, $p<0.05$, *t* test; WT+OVA-beads MFI: 133±11 vs *Irgm3−/−*+OVA-beads MFI: 78±13, $p<0.001$, *t* test). (C) Bodipy FACS analysis of CD11c+CD8+ and CD11c+CD8− splenic DCs from WT or *Irgm3−/−* untreated or 12 hours after an intravenous injection of 50μg polyI:C. Histogram plots represent activated CD11c+CD8+ (upper panel) and CD11c+CD8− (lower panel) from WT (black) and *Irgm3−/−* (red) mice. Mean fluorescence intensity values of Bodipy staining from three independent experiments were normalized to the WT untreated CD11c+CD8+ population and plotted as the average ± SEM (CD8+ WT = 100±3.9, CD8+ Irgm3−/−=82.5 ±7.5, CD8− WT=63.1±2.6, CD8−Irgm3−/−=48.5±4.1, CD8+ WT +polyI:C=132.3±11, CD8 + Irgm3−/−+polyI:C = 79.4±8.2, CD8− WT+polyI:C=79.2±6.7, CD8−Irgm3−/−+polyI:C =45.2±5.1, *t* test).

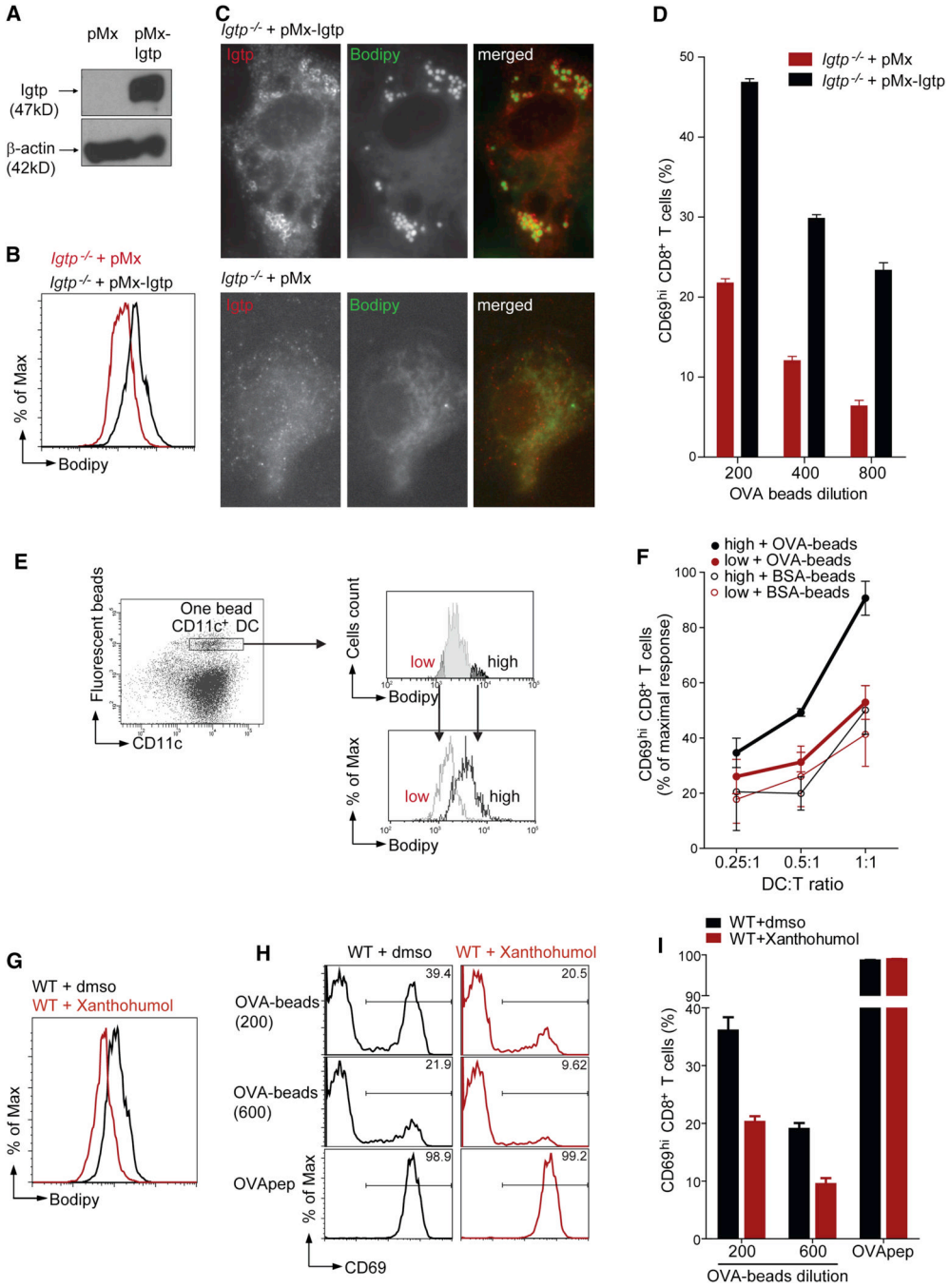

Figure 6. A role for LBs in cross-presentation

(A–D) Restoration of LB accumulation and cross-presentation by Irgm3 complementation in Irgm3−/−mDCs

Differentiated *Irgm3*−/− mDCs were infected with pMx control retrovirus or pMx-Irgm3.

(A) IB from cell lysate after 24 hour culture.

(B) FACS analysis after overnight culture of infected DCs using CD11c and Bodipy staining.

(C) IF with anti- Irgm3 staining and the LB specific Bodipy probe.

(D) Cross-presentation assay using *Irgm3*−/− mDCs infected after OVA-beads uptake with pMx or pMx-Irgm3. mDCs were extensively washed and cultured with anti-OVA OT-I CD8 + T cells. Cross-presentation was monitored by CD69 upregulation. Results are plotted ± SEM.

(E, F) Efficient cross-presentation is retained within the lipid body high fraction of WT mDCs
WT DCs having phagocytosed one bead were sorted according to their Bodipy signal, in order to obtain two DC populations, the Bodipy “high” (black line) and the Bodipy “low” (gray line), which present distinct LB accumulation.
(F) *In vitro* cross-presentation of OVA or BSA coated beads in Bodipy high and low DC populations was measured for different DC:T cells ratio. Cross-presentation was monitored by CD69 upregulation. The average of three independent experiments, each one normalized to maximal OT-I response is shown (average ± SEM).
(G– I) Pharmacological inhibition of lipid bodies inhibit cross-presentation in WT cells
(G) Bodipy staining after gating on CD11c+ cells of mDCs treated during four hours with 85 μM Xanthohumol or the control concentration of DMSO.
(H) CD69 plot after gating on Vα2+CD8+ of OT-I cells cultured overnight with fixed mDCs exposed to DMSO or 85 μM Xanthohumol during four hours after Ag uptake.
(I) Quantification of OT-I T cell activation (average ± SEM).

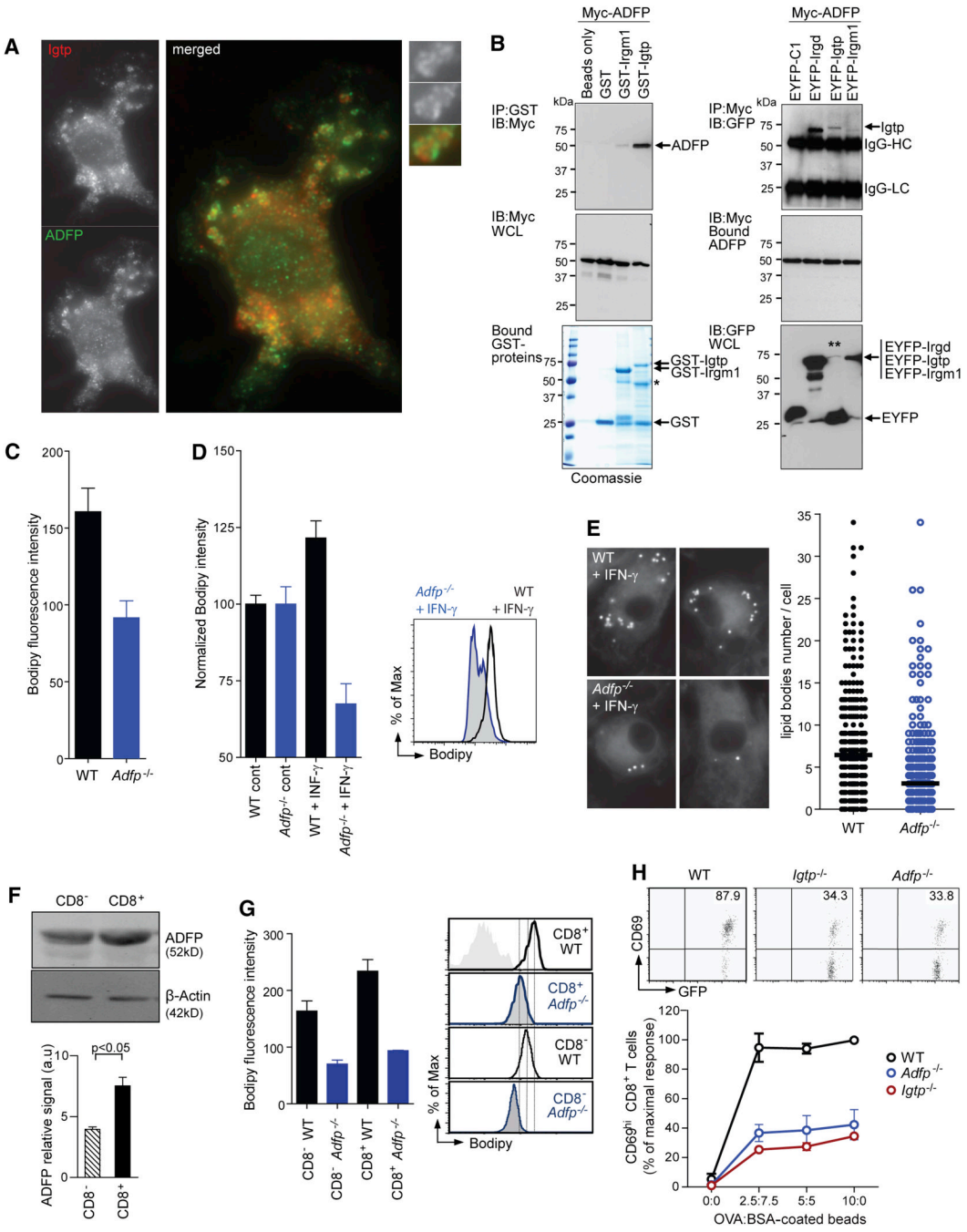

Figure 7. ADRP interacts with Irgm3 and controls LB formation and cross-presentation

(A) IF of WT mDCs treated with IFN-γ fixed and stained for Irgm3 (red) and ADRP (green). (B) Left: Immunoblot (IB) of ADRP interactions with recombinant GST-Irgm3 and another p47 GTPase, GST-Irgm1, pre-bound to glutathione-Sepaharose 4B beads. GST and beads alone served as negative controls. Comparable levels of Myc-ADRP expression in HEK whole cell lysates (WCL, middle panel) before incubation with purified GST-tagged proteins pre-bound to Sepharose beads (bottom panel). Single asterisk denotes position of cleaved GST-Irgm3 in addition to the full-length protein after bead incubation. One of two experiments is shown. Right: Co-immunoprecipitation of Irgm3 with ADRP in human HEK cells. IB of EYFP-Irgm3 retrieved by Myc-ADRP on Protein G resin. EYFP-Irgd and EYFP-C1 were used as

positive and negative controls, respectively (top panel). Double asterisk denotes low levels of full-length EYFP-Irgm3 due to instability in whole cell lysates (bottom panel). IgG-HC, immunoglobulin G heavy chain; IgG-LC, immunoglobulin G light chain. One of four similar experiments is shown.

(C) FACS analysis after Bodipy staining of non activated CD11c+ mDCs from WT or *Adrp* −/− mice (WT=160.6±15.3; *Adrp*−/−=91.6±15.3, p<0.05).

(D, E) LB quantification in WT or *Adrp*−/− mDCs treated with IFN-γ using Bodipy staining and FACS analysis (D) or LB counting by IF (E). In (D), results are normalized to 100 in the control cells (WT+IFN-γ=121.5±5.6, *Adrp*−/−+IFN-γ=67.5±6.6, p<0.0001, *t* test). An example of FACS analysis is shown. In (E), IFN-γ activated cells were submitted to LB counting by IF (WT+IFN-γ=6.44±0.36 n=372, *Adrp*−/−+IFN-γ=3.38±0.36, n=393, p<0.0001, *t* test).

(F) IB analysis of ADRP expression in cell lysates from CD8− and CD8+ spleen DC subsets. Densitometric quantification of ADRP signal intensity rapported to the β-actin loading control (three independent experiments ± SEM, statistical significance was assessed by *t* test).

(G) FACS analysis of splenic DC subsets from WT or *Adrp*−/− mice. Representative FACS fluorescence histograms of splenic CD11c+CD8− and CD11c+CD8+ subsets stained with Bodipy from WT (black lines), *Adrp*−/− (blue lines). Mean fluorescence intensity values from three independent experiments were plotted as the average ± SEM. (WT CD8−=163.7±18, *Adrp*−/−CD8−=70.17±7, p<0.01, WT CD8+=234±20, *Adrp*−/−CD8+=93.57±1, p<0.005 *t* test).

(H) *In vitro* cross-presentation of OVA- coated beads by CD11c+ spleen DCs from WT (black), *Irgm3*−/− (red) and *Adrp*−/− (blue). Cross-presentation is monitored by CD69 upregulation in anti-OVA OT-I CD8+ T cells in three independent experiments, each one normalized to the maximal OT-I response (mean ± SEM).